Laponite Nanoclay-Modified Sacrificial Composite Ink for Perfusable Channel Creation via Embedded 3D Printing

Bing Ren[1], Kaidong Song[1], Yunxia Chen[1], Walter Lee Murfee[2], Yong Huang[1,]*

[1] Department of Mechanical and Aerospace Engineering, University of Florida, Gainesville, Florida 32611, USA

[2] Department of Biomedical Engineering, University of Florida, Gainesville, Florida 32611, USA

[*] Corresponding author: Department of Mechanical and Aerospace Engineering, University of Florida, Gainesville, FL 32611, USA, Phone: 001-352-392-5520, Fax: 001-352-392-7303, Email: yongh@ufl.edu

Keywords: Embedded printing, sacrificial composite ink, Laponite nanoclay, perfusable channels, tissue engineering

Abstract

Vascularization is a major hurdle in developing *in vitro* thick tissue constructs. Fortunately, embedded sacrificial printing has emerged as a promising technology to fabricate perfusable channels. The objective of this study is to develop a Laponite nanoclay-modified polyvinyl alcohol (PVA) sacrificial composite ink that has improved printability, minimized interdiffusivity, and satisfactory post-printing removability during embedded printing of perfusable channels. With the addition of Laponite nanoclay, not only the printability of the PVA-Laponite nanoclay composite ink is significantly improved, but also the interdiffusion between the gelatin precursor solution and the PVA-Laponite nanoclay composite ink is largely mitigated. The diffusion of the gelatin

precursor solution into the PVA-Laponite nanoclay composite ink is of great importance for printing controllable perfusable channels since the diffused gelatin may cross-link as the gelatin composite matrix does during and after printing, resulting in residual gelatin gel in the channel and altered channel dimensions. In particular, the PVA-2.0% Laponite nanoclay sacrificial ink shows good printability and minimized interdiffusivity while maintaining good post-printing removability, which can be a good sacrificial composite ink for thick perfusable tissue creations. The channel diameter reduction due to the gelatin solution diffusion can be satisfactorily predicted based on the unidirectional diffusion model. This study further demonstrates the feasibility of using the proposed sacrificial ink for vascular tissue engineering applications.

1. Introduction

Organized vessel networks in thick tissues are indispensable to delivering sufficient nutrition and oxygen to the cells due to the diffusion limit (100-200 μm) [1, 2], and the creation of perfusable channel structures is the first step towards the engineering goal of the fabrication of thick vascularized tissues [3]. Perfusable channels can be engineered by casting and channel printing. During the casting approach, preformed objects (e.g., stainless steel needle or Nylon strand) [4-6] and sacrificial patterns (fabricated by molding [7, 8], and three-dimensional (3D) printing [9-12]) have been used as the patterns for the casting of matrix hydrogel subsequently. The pattern is removed after the cast hydrogel is cross-linked, thus forming perfusable channel(s). However, to realize complicated perfusable channels such as vasculature-like networks in a 3D thick-tissue space, the casting approach requires complex molds for pattern molding or a high printing resolution for pattern printing. In addition, the resulting pattern should be able to survive from hydrogel flushing during subsequent matrix hydrogel casting. Due to the aforementioned

limitations, it is still challenging to widely apply the casting approach to creating perfusable constructs.

Fortunately, 3D bioprinting [13, 14] has emerged as a promising alternative for the fabrication of thick tissue constructs with perfusable channels. Technically, 3D perfusable channels can be fabricated by 1) the positive channel printing approach that refers to the direct creation of a sacrificial channel pattern in a cross-linkable or cross-linked hydrogel matrix, in which the sacrificial pattern defines perfusable channels to be formed, and 2) the negative printing strategy, during which a matrix is selectively cross-linked while part of the matrix material as spatially defined by the designed channel pattern is not cross-linked and removed later to form a perfusable channel. Positive channel printing can be realized by sequential sacrificial printing [15, 16], photoablation [17], photodegradation [18], and embedded sacrificial printing [19-22]. During sequential sacrificial printing, the sacrificial patterns and hydrogel matrix materials are printed sequentially on each layer, and the process repeats layer by layer to form a 3D construct, followed by the removal of the embedded sacrificial materials after the cross-linking of the printed hydrogel matrix. However, the alternant printing of the sacrificial and hydrogel matrix material makes this approach laborious and challengeable to be automatic. In addition, the layer-by-layer forming fashion may introduce the interface cracks between two adjacent layers. During photoablation and photodegradation, a focalized laser beam is used to selectively break down the covalent bonds in the hydrogel matrix based on the channel design, and perfusable channels are formed after the removal of laser-processed hydrogel; however, the use of high energy lasers may cause unnecessary damage to neighboring living cells in the matrix . Alternatively, embedded sacrificial printing in a hydrogel matrix has been developed to solve the aforementioned challenges. In this

approach, the hydrogel matrix bath is a yield-stress material that allows the translation of a printing nozzle inside it and self-heals in the wake of the nozzle. Due to the yield-stress fluid property of such a hydrogel matrix bath, the deposited ink can be supported by the bath, allowing it to form a 3D structure in a free-forming fashion and maintain the shape instead of following the typical layer-by-layer solidification method. In comparison with the conventional direct ink writing method, this embedded printing method enables the printing of soft cellular materials (e.g., low viscosity, low elastic modulus) and highly intricate structures (e.g., overhang and dangling structures). It is noted that free-standing vascular/tubular structures can be printed using various 3D printing approaches such as direct ink writing, which serve a different application scenario from that of thick perfusable/vascularized tissues. In addition to positive printing strategies, negative printing strategies include various light-assisted approaches, such as stereolithography (SLA) [23] and digital light processing (DLP) [24], in which the hydrogel matrix is selectively photo cross-linked layer by layer under photonic energy while the channel pattern is uncross-linked, and perfusable channels are formed after removing the uncross-linked hydrogel. However, ultraviolet (UV) light may injure living cells embedded in the hydrogel matrix. Currently, embedded sacrificial printing has been considered one of the most promising technologies for the creation of perfusable constructs. As such, the development of good sacrificial materials for embedded sacrificial printing is also of growing interest.

For a sacrificial material to be suitable for perfusable channel creation applications using embedded sacrificial printing (or shortened as embedded printing in this study), several requirements need to be satisfied. First, it must be biocompatible to avoid cytotoxicity during and after printing. Second, it should be easily printed into a well-defined pattern as designed, which

can be retained and has limited diffusion to and from the surrounding matrix bath. Specific rheological properties such as shear-thinning and yield-stress fluid properties are usually preferred for good printability. Third, it should be easily removed from the matrix bath after the printing and cross-linking processes are completed. Mild removal conditions without compromising the structure fidelity and cell viability are also favorable. Several sacrificial materials have been identified for various bioprinting applications, which can be mainly categorized as 1) thermo-reversible materials such as Pluronic F-127 [9, 11], gelatin [15, 16, 25], and petroleum jelly-liquid paraffin [26], 2) water-soluble or water-miscible materials such as carbohydrate glass [10, 27], agarose [28], polyvinyl alcohol (PVA) (in a solid state [8, 12, 29]), and methylcellulose (MC) (as paste [30]), 3) chemically dissolvable materials such as alginate [31], and 4) mechanically extractable materials such as polydimethylsiloxane (PDMS) [32]) based on their post-printing removal mechanism. However, their use in embedded printing is yet to be further investigated. Pluronic F-127 has been reported with good shape fidelity during embedded printing and good post-printing removability (by cooling down to liquefy deposited Pluronic F-127) for perfusable channel creation [9, 19]. However, as Pluronic F-127 may be cytotoxic [33], its diffusion into the cell-laden matrix bath during the printing and removal processes could result in cell dysfunction when its concentration is too high and/or the contact time is too long. Carbohydrate glass, agarose, and PVA require an elevated printing temperature (>80°C) to melt and print them, and printing at elevated temperatures is usually implemented for the pattern printing-then-casting approach but unsuitable for embedded printing due to possible thermal injuries to living cells in the matrix bath. While gelatin, PVA, and MC may be prepared into solutions and printed as aqueous sacrificial inks during embedded printing [15, 16, 19, 25], there is only a limited range of viscosity that is feasible for printing due to their insignificant shear-shinning properties, and their aqueous property

leads to serious interdiffusion with the hydrophilic matrix bath after their deposition. The interdiffusion further affects the printing resolution and final channel geometry. Alginate needs to be removed using chelating agents such as sodium citrate or ethylenediaminetetraacetic acid (EDTA), but the chelators may inhibit the cell viability [34]. PDMS and petroleum jelly-liquid paraffin have also been used as sacrificial inks for channel fabrication, but the curing of PDMS filaments and liquefying of the petroleum jelly-liquid paraffin after printing requires an elevated temperature (80℃ for PDMS [32] and 70℃ for petroleum jelly-liquid paraffin [26]), which forbidden the cell incorporation into the matrix. Therefore, the adoption of such sacrificial inks for channel creation by embedded printing is still constrained by the need for better printing qualities, and there is a great need to develop a better ink for embedded sacrificial printing.

The objective of this study is to develop a Laponite nanoclay-modified PVA sacrificial composite ink with improved printability, minimized interfacial diffusion and maintaining satisfactory post-printing removability during embedded printing of perfusable channels. PVA is chosen as a model sacrificial material in this study for its good biocompatibility [12, 29, 35] and water solubility but bad printability during embedded printing. Laponite nanoclay ($Na_{0.7}Si_8Mg_{5.5}Li_{0.3}O_{20}(OH)_4$), a nanoscale ceramic disc with a diameter of ~25 nm and a thickness of ~1 nm, is known as a biocompatible [36-38] rheology modifier that can enhance the interactions with the polymer chains when mixed with various hydrogels [39-41] to improve the ink printability during conventional extrusion printing. In this study, the Laponite nanoclay is added to enhance the PVA ink printability while mitigating the post-printing interfacial diffusion when embedded printing. Specifically, the interdiffusion between the PVA aqueous solution, which doesn't experience any sol-gel phase change during printing, and typical hydrogel-based matrix bathes is mitigated by the

addition of Laponite nanoclay. In summary, the sacrificial composite ink is designed by adding Laponite nanoclay into an aqueous PVA solution to improve the ink printability and minimize the interdiffusion between the ink and matrix bath without deteriorating the ink biocompatibility or removability during embedded printing.

2. Materials and Methods

2.1. Laponite nanoclay-modified PVA sacrificial composite ink preparation

PVA powders (molecular weight ~22,000 g/mol, degree of hydrolysis 88%, MP Biomedicals, Solon, OH, USA) were swelled in deionized (DI) water at 70°C for 1 h and then fully dissolved by heating up to 95°C for 1 h to obtain the 40% w/v PVA solution. Laponite nanoclay XLG powders (BYK Additives, Inc., Gonzales, TX) were suspended in DI water with a concentration of 2% and 4% w/v and mixed for 1 min using a centrifugal mixer (AR-100, Thinky, CA, USA). The resultant Laponite suspension was allowed to sit for at least 20 min until it was physically gelled. Then the Laponite suspension was mixed with the 40% w/v PVA solution with a volume ratio of 1:1 using the centrifugal mixer for 1 min to obtain the 1% and 2% w/v Laponite nanoclay composite inks with 20% w/v PVA as the scaffold polymer. To get the homogeneous composite, the inks were transferred to 50 mL centrifuge tubes and placed on a roller (MX-T6-S, DLAB, Beijing, China) for rolling overnight. For comparison, a 20% w/v pure PVA solution was also prepared without any addition of Laponite nanoclay. For better sacrificial ink extrusion and post-printing ink removal, the Laponite nanoclay concentration higher than 2% was not investigated.

2.2. Gelatin microgel-gelatin solution composite matrix bath preparation

The gelatin microgel-gelatin solution composite matrix bath (shortened as gelatin composite

matrix) functions as the support media during embedded printing and was first prepared as described previously [19, 21]. Briefly, a 10% w/v gelatin solution was prepared by dissolving gelatin type A powders (225 bloom, MP Biomedicals, Solon, OH, USA) in Dulbecco's phosphate-buffered saline (dPBS, Corning cellgro Manassas, VA, USA) at 37°C for 30 min. Transglutaminase (TG, Modernist Pantry, York, ME, USA) solution (200 mg/mL) was prepared by dissolving the lyophilized powder at 37 °C for 37 min in dPBS and added into the gelatin solution with a volume ratio of 1:19 to have a final TG concentration of 10 mg/mL. Then, the gelatin solution was cross-linked by TG at 37°C for 24 h. The cross-linked gelatin gel was deactivated by boiling for 30 min, followed by breaking up into microgels using a 3-speed hand blender (KitchenAid, Benton Harbor, MI, USA) for 5 min. The microgels were collected and centrifuged for 5 min at 4200 rpm to remove the water supernatant. Finally, 3% w/v gelatin type A powders were added into the gelatin microgel tube and dissolved for 30 minutes at 37°C before printing. The prepared gelatin composite matrix contains two homogeneously distributed phases, a discrete phase of gelatin microgels and a continuous phase of gelatin precursor solution that can be further cross-linked by TG. This tailored composition of mixed phases gives the gelatin composite matrix a yield-stress fluid property, which enables the translation of the nozzle and self-recovery in the wake of the nozzle during the embedded printing process. The gelatin composite matrix cross-links under the effect of TG during and after printing [19, 42], resulting in a gel structure.

2.3. Rheological properties characterization

To characterize the rheological properties of the prepared PVA-Laponite nanoclay composite inks, the viscosity, shear stress, and shear moduli (storage modulus G' and loss modulus G") were

measured by steady rate sweeps using a rheometer (MCR-702 TwinDrive, Anton-Paar, Graz, Austria) as described previously [43]. Specifically, steady rate sweeps were performed at a strain of 1.0% with a shear rate range from 0.01 to 100.00 s^{-1}.

2.4. Extrusion of sacrificial inks in bath and filament morphology characterization

Sacrificial inks were manually extruded downwards in the gelatin composite matrix bath using a glass syringe (inner diameter of 0.41 mm, Hamilton, Reno, Nevada, USA) on a tensiometer (Attension ThetaLite 101, Biolin Scientific, AB, Sweden), while the nozzle outlet was fixed about 10 mm below the bath surface. Around 2 μL of the ink materials were extruded into the gelatin composite bath, while both the nozzle and bath remained static, ensuring the results were not affected by the printing speed. For morphology characterization of the extruded filaments, pictures of the extruded inks were taken using the tensiometer and further processed using ImageJ (NIH, USA).

2.5. Embedded printing and perfusable channel creation

The printing study was performed using a pneumatic 3D bioprinter (Cellink Inkredible, Boston, MA, USA) with a general-purpose gauge 22 dispensing tip (inner diameter of 0.41 mm, Nordson EFD, East Providence, RI, USA). Several two-dimensional (2D) and 3D patterns were designed using SolidWorks (Dassault Systemes SolidWorks Corp., Waltham, MA, USA), and their G-codes were manually programmed for printing path control. Before printing, the 200 mg/mL TG solution was added into the gelatin composite matrix (volume ratio = 1:19) to have a final TG concentration of 10 mg/mL to initiate the cross-linking process of the gelation solution phase. The resultant homogeneous matrix was cast into a customized PDMS container for instant embedded printing,

and PVA-Laponite nanoclay (with 0%, 1%, and 2% w/v nanoclay, respectively) composite inks were used as the sacrificial inks. For perfusable channel creation, the effects of extrusion pressure (60-120 kPa) and path speed (0.5-4 mm/s) on the created channel diameter were investigated. Each printed construct was incubated at 37 °C for around 45 min, and then the cross-linked construct was immersed in dPBS for 15 min - 1 h (depending on the complexity of the sacrificial pattern(s)) until the sacrificial PVA-Laponite ink was fully diluted to be much less viscous, followed by gently flushing using a syringe.

2.6. Inter-diffusion characterization

PVA-Laponite nanoclay (0.5%, 1.0%, 1.5%, and 2.0% w/v nanoclay, respectively) composite inks were used to measure the final channel diameter and estimate the gelatin diffusion profile from the gelatin composite matrix to the sacrificial ink. For better visualization during post-printing diffusion tests, 0.1% w/v Rhodamine 6G (Acros Organics, NJ, USA) was added into the gelatin composite matrix, and images were taken using a fluorescence microscope (EVOS, ThermoFisher Scientific, Waltham, MA, USA). The gelatin diffusion coefficient D was determined using the Einstein-Smoluchowski equation:

$$D = L^2/2t \tag{1}$$

where L is the diffusion distance, which was measured from the static fluorescent images taken every 5 min in a 2-hour period, and t is the time. The gelatin diffusion profile was then characterized by the unidirectional diffusion equation:

$$C_{(x,t)} = C_0\left[1 - erf\left(\frac{x}{\sqrt{2Dt}}\right)\right] \tag{2}$$

where $C_{(x,t)}$ is the gelatin concentration at the radial position of x and time t, C_0 is the initial gelatin concentration (3.0% w/v in this study), and *erf (-)* is the error function.

2.6. Cell culture

To evaluate the efficiency of printed perfusable channels in supporting the mass transport of sufficient nutrients and oxygen to the surrounding matrix, NIH 3T3 mouse fibroblasts (ATCC, Rockville, MD) in a gelatin composite matrix were dynamically cultured via a printed perfusion channel. The gelatin microgel-gelatin solution composite matrix bath was prepared as aforementioned. Specifically, 3% w/v gelatin type A powders were mixed with the pre-made gelatin microgels and fully dissolved for at least 30 min at 37°C. 1M NaOH was used to tune the matrix to a pH of 7.4. Then, 3T3 cells were gently mixed into the gelatin composite matrix to have a cell concentration of 3×10^6 cells/mL. Before embedded sacrificial printing, the 200 mg/mL TG solution was added into the cellular gelatin composite matrix (volume ratio = 1:19) to have a final TG concentration of 10 mg/mL and gently mixed. The resultant homogeneous cellular matrix was cast into a customized rectangular PDMS cell culture chamber to have a size of 6 mm× 4 mm× 4 mm for embedded sacrificial printing with the PVA-2% Laponite nanoclay composite ink. The printed construct was then cross-linked at 37 °C in a humidified 5% CO_2 incubator for around 45 min. After the channel was created by dissolving the sacrificial ink with the perfused dPBS solution, the culture chamber was connected to a perfusion system, and Dulbecco's modified Eagle's medium (Sigma-Aldrich, St. Louis, MO, USA) with 10% fetal bovine serum (HyClone, Logan, UT, USA) was dynamically perfused at a flow rate of 16 μL/min using a peristaltic pump (Ismatec, Wertheim, Germany). As the control group, a same-size bulk cellular gelatin composite structure but without any channels was cultured under a static cell medium condition. The same cell medium was used as that for the perfusion group but only added onto the top surface of the construct and changed every two days. After culturing for 4 days, the resulting cellular construct was taken out

from the culture chamber and sectioned into slices (perpendicular to the channel direction) by a surgical blade, and fluorescein diacetate (FDA, Sigma-Aldrich, St. Louis, MO, USA) and ethidium homodimer-1 (EthD-1, Sigma-Aldrich, St. Louis, MO, USA) were used to stain live and dead cells, respectively, in both constructs. Images were acquired using the EVOS fluorescence microscope.

3. Results and Discussion

3.1. Rheological characterization of Laponite nanoclay-modified PVA sacrificial composite inks

Certain ink rheological properties are desirable for extrusion printing. In addition to having certain viscosity, shear-thinning and yield-stress fluid properties are usually helpful for successful printing. While increasing the ink concentration is one of the possible methods to increase the ink viscosity, the shear-thinning and yield-stress fluid properties of the PVA solution remain almost the same even when the concentration increases to 40% according to preliminary experiments [19]. Fortunately, the addition of Laponite nanoclay significantly improves the ink rheological properties due to the formation of a "house-of-cards" structure arrangement driven by the positive and negative charge distribution [39]. To make the resultant ink flow, a threshold force is required to disrupt the "house-of-cards" structure, which is the cause of the ink yield stress, and the resulting composite PVA-Laponite nanoclay hydrogel colloid inherits the shear-thinning and yield-stress fluid behavior of Laponite nanoclay colloids. To be noted, it has long been predicted of the establishment of a "house-of-cards" structure in Laponite clay suspensions; unfortunately, imaging the microstructure of Laponite nanoclay discs is still a technical challenge, leaving an ongoing debate [44, 45].

Figure 1a(i-iii) shows a schematic of the design principle of the PVA-Laponite nanoclay composite ink. The PVA molecular chain (Figure 1a(i)) contains hydroxyl groups (–OH) that are likely to form hydrogen bonds with the silanol (Si–O) groups on the Laponite nanoclay surfaces (Figure 1a(ii)) [46-48]. At the same time, the Laponite nanoclay gel is then stabilized by the electrostatic interactions between the negatively charged faces and positively charged edges of disc-shaped nanoclay particles [49], resulting in a Laponite nanoclay-based house-of-cards structure connected with numerous PVA chains (Figure 1a(iii)).

As seen from Figure 1b, 20% PVA ink with 0% Laponite nanoclay shows the lowest viscosity. The viscosity of the PVA inks modified with 1% and 2% Laponite nanoclay is high at the shear rate of 0.01/s and decreases with the increase of the shear rate, which represents the typical shear-thinning property. From the shear stress-shear rate results in Figure 1c, the PVA-0% nanoclay ink is not a yield-stress fluid, while the 1% and 2% Laponite nanoclay modified inks show a good yield-stress fluid property. The rheological behavior of the PVA-Laponite nanoclay inks also indicate the good dispersion of the nanoclay discs. As seen from Figure 1d, the yield-stress values of the 1% and 2% PVA-nanoclay inks are 113.2 ± 17.5 and 492.8 ± 13.8 Pa, respectively. The 0% nanoclay composite ink shows a liquid state under the entire shear rate range investigated in this study, while the crossover points of storage modulus (G') and loss modulus (G") are observed in the PVA-1% nanoclay and PVA-2% nanoclay inks. G" starts to dominate when the shear stress surpasses the crossover point, indicating the transfer from gel-like to liquid-like behaviors. In comparison with the 1% nanoclay ink, the 2% nanoclay ink shows higher phase stability in a wide range of shear stress and a higher shear stress value at the crossover point of G' and G", indicating improved capability of sustaining higher stresses and keeping good structural integrity.

3.2. Printability evaluation of Laponite nanoclay-modified PVA sacrificial composite inks

Herein the ink printability is evaluated based on the ink spreading performance in the gelatin composite matrix. It is noted that the inks used in this study were dyed in blue but shown as grey in the imaging system. When extruded at a fixed position in the gelatin composite matrix, the 20% PVA ink with 0% Laponite nanoclay has the most significant spreading into the surrounding gelatin (or die swelling) at the printing nozzle outlet, as seen in Figure 1e(i). The ink spreading includes a diffusion process as well as a convection process upwards along the nozzle, indicating its deficiency in retaining the shape of deposited filaments/patterns. As such, it is unpractical to print a good pattern using such an ink. When mixing with 1% Laponite nanoclay, the modified PVA ink shows the improved filament shape fidelity (Figure 1e(ii)) with minor spreading. However, the deposited filament still shows a roughly spherical conformation due to the interfacial tension. In comparison, the PVA ink with 2% Laponite nanoclay shows an excellent filament morphology and shape fidelity after being extruded out of the cylindrical printing nozzle (Figure 1e(iii)). The ink spreading and spherical droplet forming phenomena observed from the PVA-0% nanoclay and PVA-1% nanoclay inks are negligible for the PVA-2% nanoclay ink. The good printability is thus expected when using the PVA-2% nanoclay ink. It is noted that the spreading is not due to the diffusion of the dye; otherwise, the diffusion should be observed in all groups.

To evaluate the extrusion performance of sacrificial inks in the gelatin composite matrix, a non-dimensional number, defined as the spreading ratio (*Sr*), is proposed to quantitively analyze the filament morphology as follows:

$$Sr = \frac{A_{actual} - A_{ideal}}{A_{ideal}} \tag{3}$$

where A_{actual} is the actual pixel area occupied by a printed ink, and A_{ideal} is the theoretical pixel area of a non-spreading ink filament, which is defined as the rectangular zone as defined by the nozzle inner diameter (shown as the dashed rectangle in Figure 1e). A smaller *Sr* means less ink spreading and up-flow, which is desirable for high-resolution embedded printing. As shown in Figure 1f, the spreading ratio value of the 0%, 1%, and 2% Laponite nanoclay-modified PVA inks is 2.5 ± 0.4, 1.0 ± 0.1, and 0.2 ± 0.1, respectively, indicating the PVA-2% nanoclay ink has the best printability. The results demonstrate the effectiveness of the Laponite nanoclay in improving the printability of PVA inks. As a demonstration, several intricate 3D patterns were designed and printed with the PVA-2% nanoclay ink in the gelatin composite bath as shown in Figure 1g, highlighting the advantages of the embedded printing strategy in generating 3D overhang structures.

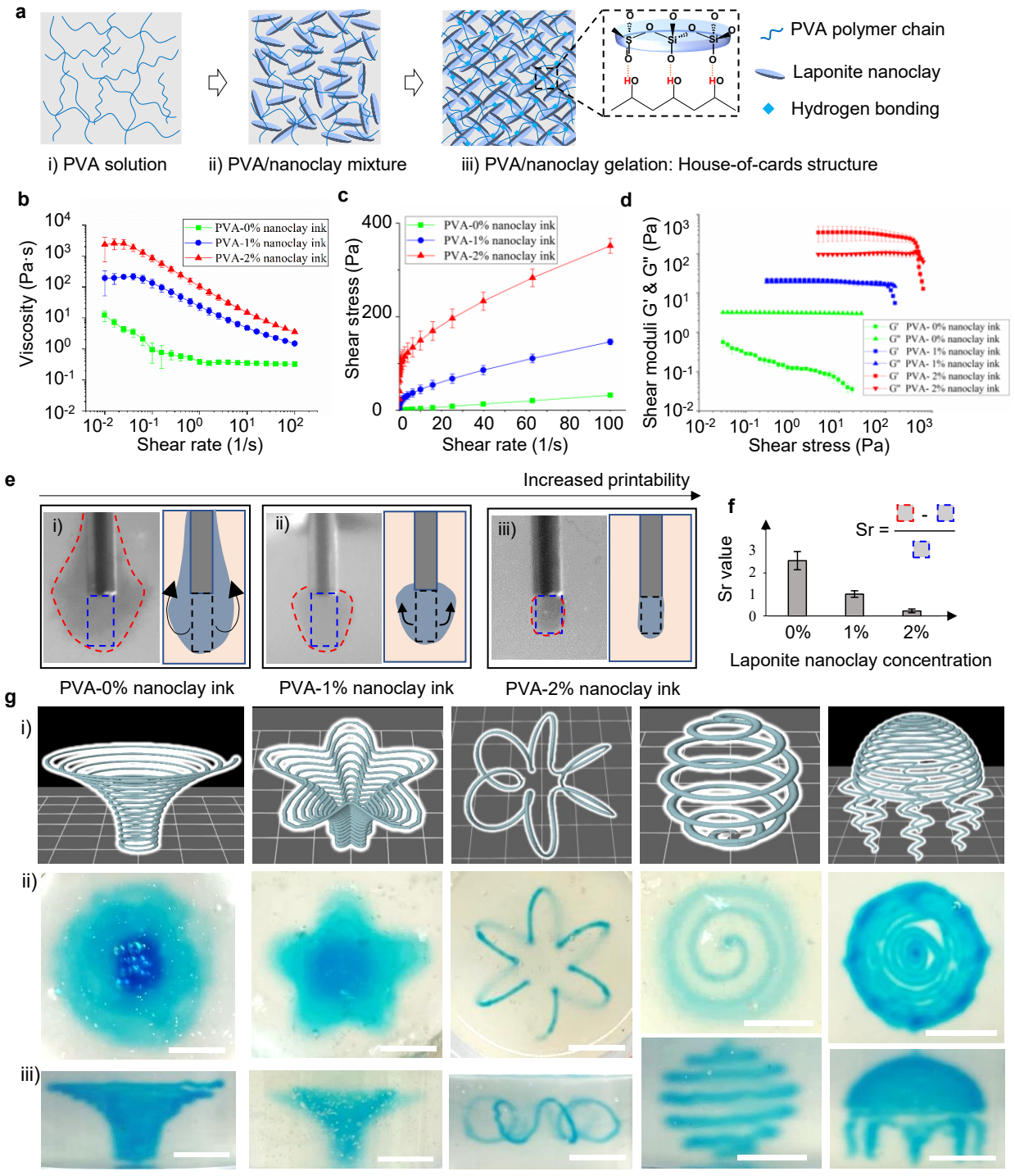

Figure 1. **(a)** Schematics showing the formulation of the Laponite nanoclay-modified PVA sacrificial composite ink. **(b-d)** Rheological characterization of the Laponite nanoclay-modified PVA inks: (b) viscosity, (c) shear stress, and (d) shear moduli. **(e)** Extrusion printing performance in the gelatin microgel-based composite matrix: i) 20% PVA-0% Laponite nanoclay, ii) 20% PVA-

1% Laponite nanoclay, and iii) 20% PVA-2% Laponite nanoclay (blue dashed lines: ideal filament shapes; red dashed lines: actual filament contours after spreading; and black arrows: spreading directions). **(f)** *Sr* value as a function of nanoclay concentration. **(g)** 3D patterns printed with 20% PVA-2% Laponite nanoclay ink in gelatin composite matrix: i) design, ii) and iii) top and side views of the printed structures. (Scale bars: 5 mm)

3.3. Creation of thick constructs with perfusable channels

Figure 2a is a schematic of the embedded printing process for perfusable channel creation. The gelatin composite matrix is first cast in the chamber to act as the matrix for embedded sacrificial printing. After the printing of sacrificial PVA-nanoclay composite ink is completed, the chamber is incubated to allow the cross-linking of the gelatin composite matrix. Finally, the sacrificial ink is diluted and flushed away from the matrix using DI water, thus forming a channel for medium perfusion. As observed, the addition of the Laponite nanoclay at low concentrations (such as 1% to 2%) does not affect the water-based removability of the original PVA ink significantly (Figure S1).

Human vasculature has a sophisticated geometry that contains repeated bifurcations and tortuosity. Ideally, engineered channels should be able to recapitulate these features of meso- and macro-sized vessels. As an illustration of the feasibility of using the PVA-2% Laponite nanoclay composite ink to fabricate perfusable channels in thick constructs, several 2D and 3D channel patterns are designed and printed in the gelatin composite matrix. Well-defined perfusable patterns such as 2D serpentine, bifurcate, crossed, 3D spiral, and other intricate designs were created (Figure 2b). The deposited sacrificial ink is removed from the gelatin composite matrix after the cross-linking process is completed, leaving channels for perfusion by dissolving and rinsing the ink with DI water. The channel diameter could be controlled by tuning the printing conditions. Figure 2d and e shows the creation of channels with different diameters by varying the extrusion

air pressure and path speed when using a fixed 410 μm diameter nozzle. The channel diameter increases from 491.4 ± 39.9 μm to 1335.1 ± 134.8 μm when the extrusion pressure increases from 60 kPa to 120 kPa at a constant path speed (1 mm/s) (Figure 2 d). At a constant extrusion pressure of 100 kPa, the increase of the path speed from 0.5 mm/s to 4.0 mm/s results in a decrease in channel diameter from 1210.4 ± 133.7 μm to 470.2 ± 66.1 μm; similarly, at a pressure of 60 kPa, the channel diameter decreases from 755.5 ± 93.7 μm to 308.7 ± 38.7 μm under the same increase in path speed (Figure 2 e-f). The change of channel diameter are well-fit (100 kPa: R^2 = 0.91; 60 kPa: R^2 = 0.97) as a function of path speed by a power-law equation with exponents of -0.47 (100 kPa) and -0.44 (60 kPa) (shown as the dashed lines in Figure 2e), which are close to the theoretical value (-0.5) according to the flow rate equation ($Q = \frac{\pi d^2}{4} v$, where Q is the flow rate, d is the filament diameter, and v is the path speed). It should be noted that even smaller channel diameters can be achieved theoretically by decreasing the extrusion pressure and/or increasing the path speed, the filament might be discontinuous or difficult to be removed due to the post-printing interdiffusion with the surrounding gelatin matrix.

For comparison, the PVA-0% Laponite nanoclay ink was also utilized to create perfusable channels but shows serious interdiffusion, so the printed pattern does not show a well-defined shape as designed (Figure 2f), and a crevice is found from the cross-sectional view. It is concluded that with the addition of Laponite nanoclay, the PVA-Laponite nanoclay composite ink offers can be successfully utilized for embedded sacrificial printing of perfusable channels.

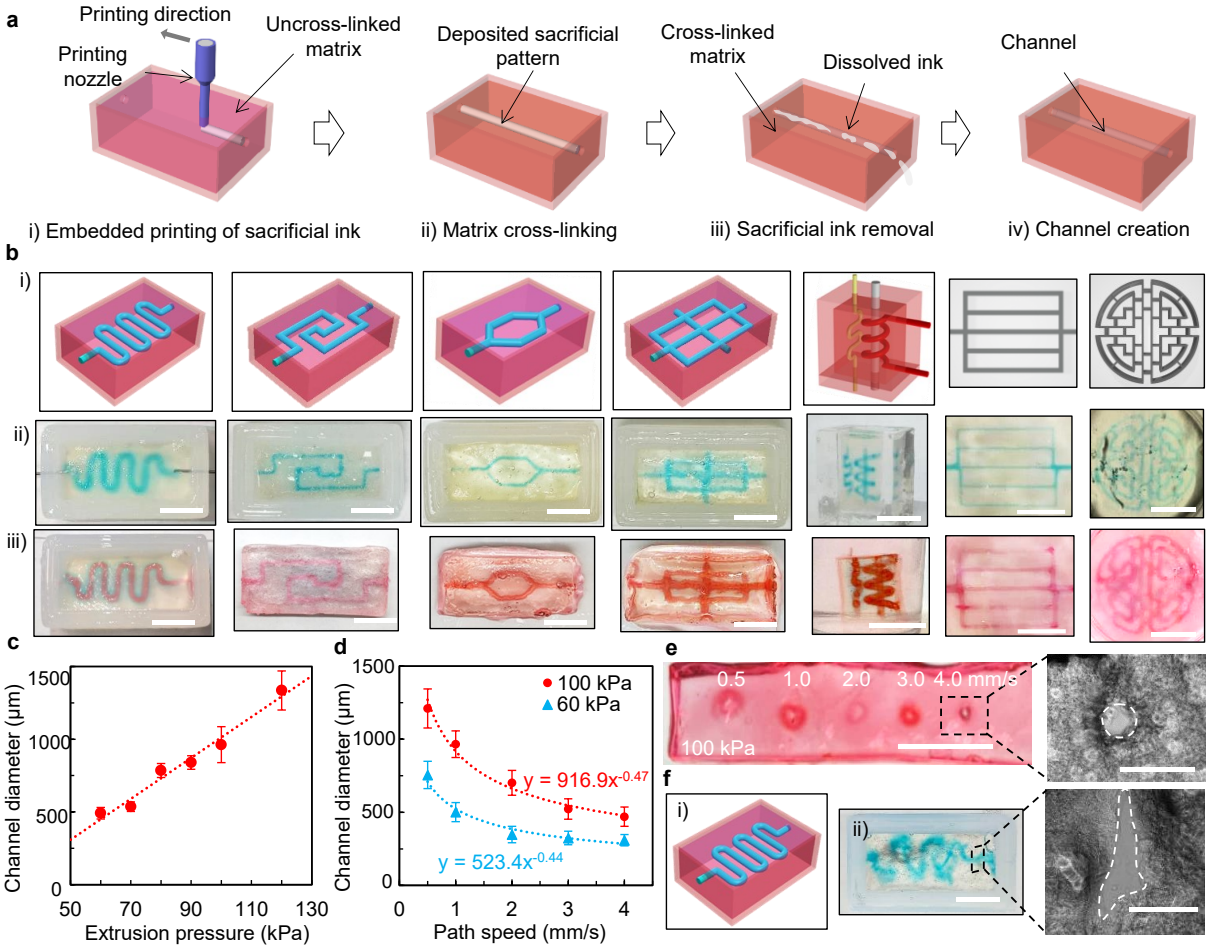

Figure 2. **(a)** Schematic of the embedded printing approach for perfusable channel creation. **(b)** Embedded printing of complex patterns and removal results of PVA-2% Laponite nanoclay ink in the gelatin composite matrix: (i) design, (ii) printed filaments (in blue), and (iii) perfusable channel formation (perfused with red dye). **(c)** Effects of extrusion pressure on the channel diameter. **(d)** Effects of path speed on the channel diameter at applied pressures of 60 kPa and 100 kPa. Dashed lines are fitted curves. **(e)** Bright-field image of the channel cross-section using path speeds of 0.5, 1.0, 2.0, 3.0, and 4.0 mm/s at 100 kPa (perfused with red dye), and (inset) a microscopy cross-sectional image of the channel created at path speed of 4.0 mm/s. **(f)** Printing results using the PVA-0% Laponite nanoclay ink: (i) design and (ii) printing results, and (inset) a microscopy cross-sectional image of the cracked channel. Scale bars: b and f(ii); e, 5 mm; e inset and f(ii) inset, 1 mm. Error bars: +/- sigma.

3.4. Dynamic cell culturing using perfusable channels

The proposed channel creation approach is further demonstrated to create thick perfusable tissues for dynamic cell culturing, and its effectiveness is evaluated based on the cell viability of 3T3 cells under dynamic perfusion. The fabricated gelatin composite structures are soft but not particularly

fragile, which exhibit an effective elastic modulus in the same range as many human tissues (0.1 kPa to 1 MPa) [21]. The printed channel is also temporally stable over the continuous fluid perfusion (Figure S2). **Figure 3**a shows the schematic of the perfusion system and actual setup. The usage of a perfusable channel created using the proposed sacrificial PVA-2% Laponite nanoclay composite ink is evaluated for dynamic perfusion culturing a thick 3T3 cell construct (6 mm×4 mm×4 mm) with the created channel at the center (Figure 3b(i)). The control is a 3T3 cell construct with the same dimensions but without any channels (Figure 3b(ii)). The cell live/dead staining results are shown in Figure 3c, where live cells are stained in green while dead cells are in red (the dead cells are only shown in the inset). As seen from Figure 3c(i), more live cells are found at the construct outskirt area surrounded by the cell medium and the circular zone nearby the perfusion channel, which is due to the medium diffusion limit in the gelatin composite matrix (around 800 μm in this study). This value is higher than the typical diffusion limit (100-200 μm) in the human body, which is probably due to the mass transport property of the gelatin composite matrix herein. Beyond the effective diffusion distance, the cell viability is significantly decreased compared to that in the area close to the channel. For the control without a perfusion channel (Figure 3c(ii)), the cell viability is low towards the inner region due to the lack of necessary cell medium.

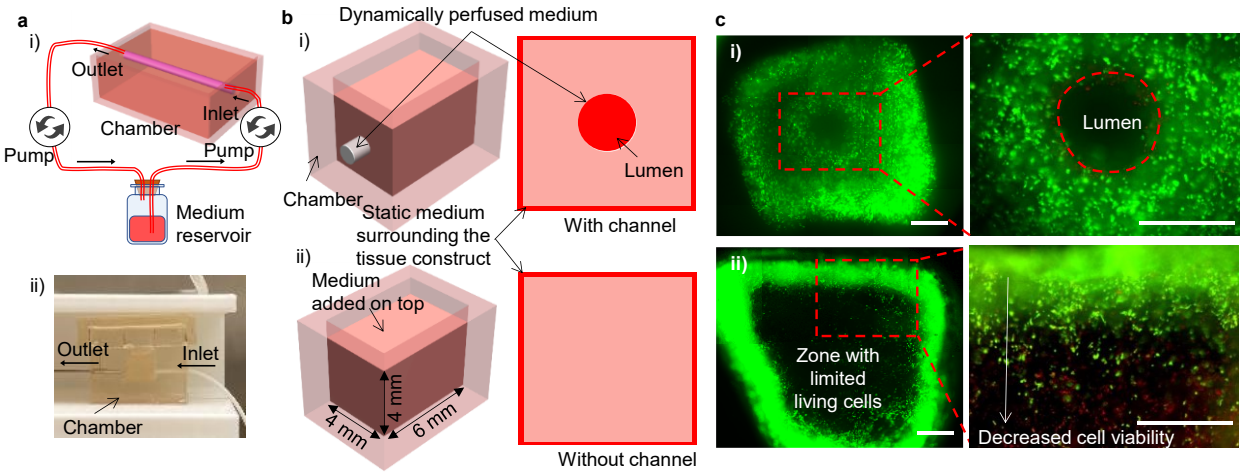

Figure 3. **(a)** Dynamic culture by continuous perfusion of cell medium through the created channel. (i) Schematic of the perfusion system and (ii) the cell culture chamber being perfused. **(b)** Designs of the cell culture chambers (i) with channel and (ii) without channel, and **(c)** fluorescent live/dead images of 3T3 cells cultured after 4 days (i) with channel and (ii) without channel. (Scale bars: 1 mm.)

4. Discussion on Post-printing Interfacial Diffusion

During aqueous-in-aqueous printing, the interdiffusion between the aqueous sacrificial ink and aqueous matrix bath cannot be ignored in precisely creating perfusion channels. In this study, the gelatin composite matrix is composed of gelatin microgels and a gelatin precursor solution. After deposition of the sacrificial PVA-nanoclay composite ink (**Figure 4**a(i)), a bi-directional diffusion happens between the aqueous PVA and the gelatin solution of the matrix bath as illustrated in Figure 4a since both are hydrophilic and miscible. As the interdiffusion proceeds, the polymer chains on both sides begin to transport towards each other in a fashion of bi-directional diffusion. As a result, the interface between the originally printed filament and gelatin composite matrix diminishes, gradually replaced by an interdiffusion layer. This interdiffusion layer consists of PVA and gelatin chain entanglements newly established due to the intermixing of the sacrificial ink and gelatin precursor solution. The thickness and strength of the interdiffusion layer increase with time, which is attributed to the ongoing penetration and interlacing of the PVA and gelatin chains across

the interface. Finally, a cannular interdiffusion layer is formed around the original filament outskirt region (Figure 4a(ii)). It should be noted that the diffusion of the matrix material (gelatin) into the sacrificial composite ink may result in incomplete removal of the sacrificial ink because of the diffused gelatin precursor solution in the PVA-nanoclay filament. If the concentration of the diffused gelatin is high enough, it may gel and bond with part of the sacrificial ink (Figure 4a(iii)) and turns to be not removable, resulting in channels with a smaller diameter than that of printed filaments.

As observed, the addition of Laponite nanoclay can not only reduce the diffusion of PVA into the matrix bath, but also reduce the diffusion of gelatin precursor into the PVA ink. Figure 4b shows the cross sections of the formed channels after the removal of the sacrificial inks. The PVA chains of the PVA-0% nanoclay ink transport pronouncedly into the surrounding gelatin composite matrix. During the translation of the printing nozzle, the volume in the wake of the nozzle is disturbed and liquefied to be liquid-like due to the yield-stress fluid property of the gelatin composite matrix. This further promotes the mass transport rate between the PVA ink and gelatin solution along the vertical direction as seen as a crevice through the top surface (Figure 4b(i)). The inks with the Laponite nanoclay additive show reduced interdiffusion and improved shape fidelity, and both PVA and gelatin diffusion is reduced to a certain degree. The channels with a round lumen morphology (blue dashed lines in Figure 4b(ii) and (iii)) can be created for both 20% PVA-1% and 20% PVA-2% Laponite nanoclay inks. In particular, the 20% PVA-1% Laponite nanoclay ink has a smaller residual interdiffusion layer thickness after the sacrificial ink removal while the PVA diffusion into the matrix bath is also less pronounced. The results indicate that the addition of the Laponite nanoclay helps reduce the ink/matrix interdiffusion and better retain the designed channel

geometry after the removal of sacrificial inks. As shown in Figure 4c, the final channel diameter increases with the nanoclay concentration and thus becomes closer to the designed value (650 μm for this study), which is due to the suppressed gelatin precursor diffusion into the sacrificial inks.

Using the Einstein-Smoluchowski equation, the diffusion coefficient of gelatin precursor is determined from the plot of L^2 as a function of time t (Figure 4d). Specifically, the diffusion coefficients of gelatin solution when printing with the PVA ink and 0.5%, 1.0%, 1.5%, and 2.0% nanoclay are 1.08×10^{-11}, 6.35×10^{-12}, 3.62×10^{-12}, and 4.71×10^{-13} m^2/s, respectively. The gelatin concentration decreases toward the middle of the ink along the radial direction (at t = 10 min), and its profile is predicted based on the estimated diffusion coefficients and shown in Figure 4e (based on the unidirectional diffusion model). At a specific radial distance, a lower concentration of nanoclay ink has a higher diffused gelatin solution concentration, which may cause difficulty for ink removal after the gelatin solution is cross-linked. In comparison, the PVA-2.0% nanoclay ink shows the least gelatin diffusion from the matrix to result in the formation of unremovable gelatin gel (around 26.8 μm) if the 0.8% gelatin solution concentration is used as a threshold for gelatin removable or not during the sacrificial ink removal step. The radial thickness of this unremovable gelatin gel is smaller than those when using the other PVA inks with 0.5%, 1.0%, and 1.5% Laponite nanoclay as predicted as seen from Figure 4e (126.6 μm, 96.7 μm, and 73.2 μm, respectively), which is helpful to keep the original channel diameter. As seen from Figure 4c, the average final channel diameter is 389.5 μm, 423.9 μm, 515.6 μm, and 591.4 μm for the PVA inks with 0.5%, 1.0%, 1.5%, and 2.0% nanoclay, respectively. As such, the difference between the original filament and final perfusable channel is 260.5 μm, 226.1 μm, 134.4 μm, and 58.6 μm, respectively, and the corresponding reduction of the channel radius matches satisfactorily with the

thickness of diffused gelatin-induced gel as predicted (130.3 vs. 126.6 μm, 113.1 vs. 96.7 μm, 67.2 vs. 73.2, and 29.3 vs. 26.8 μm for the PVA inks with 0.5%, 1.0%, 1.5%, and 2.0% nanoclay, respectively).

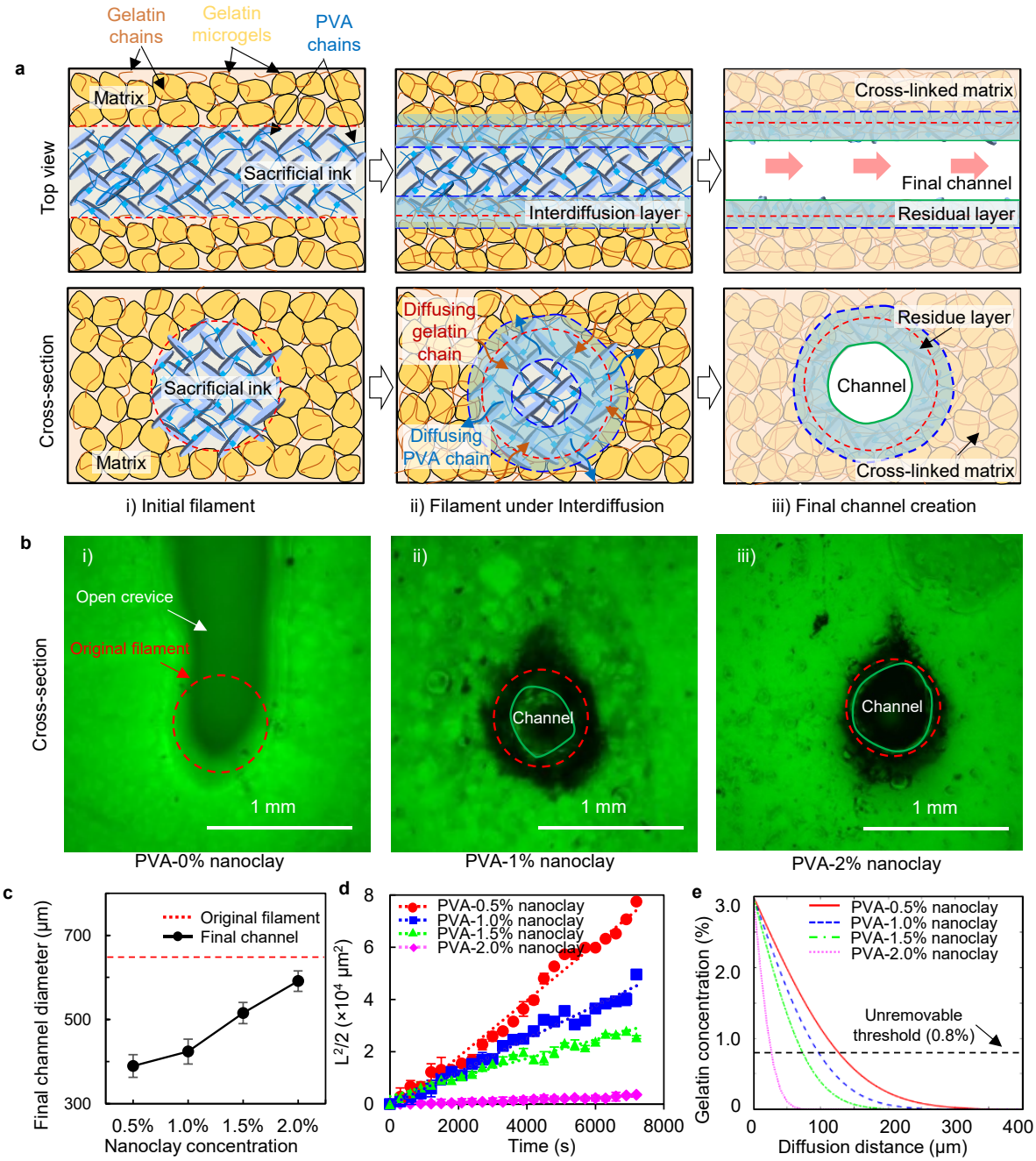

Figure 4. **(a)** Schematics and **(b)** images of the interdiffusion between the composite sacrificial ink and gelatin composite matrix. For (a), red dashed lines/circles illustrate the original filament contours as printed, blue dashed lines/circles illustrate the diffusion fronts of the PVA and gelatin

chains, green solid lines/circles illustrate the final channel contours, and the sacrificial ink, interdiffusion layer, and residual interdiffusion layer are marked using a curly bracket to their right, respectively. For (b), red dashed circles illustrate the original filament contours as printed and green solid circles illustrate the final channel contours. The black cannular patterns in (b)(ii) and (b)(iii) are the residual interdiffusion layers. **(c)** Final channel diameter after removal of the sacrificial ink. **(d)** Plot of L^2 as a function of time t, and the diffusion coefficient D is determined from the slope. **(e)** Gelatin diffusion profile along the radial distance (at t = 10 min).

5. Conclusions and future work

The feasibility of using Laponite nanoclay as an additive for the preparation of sacrificial composite ink has been evaluated for the embedded sacrificial printing of thick perfusable constructs. Specifically, the printability, channel creation, and interdiffusivity have been studied using the Laponite nanoclay-modified composite ink. The PVA solution is selected as a base sacrificial ink for its good water removability but limited printability under room temperature. With the addition of Laponite nanoclay, the PVA-Laponite nanoclay composite ink shows improved filament formability, indicating that the Laponite nanoclay improves the ink printability and shape fidelity. This is especially beneficial for sacrificial inks with poor rheological properties. More importantly, the addition of Laponite nanoclay reduces interdiffusivity between the PVA-Laponite composite ink between the matrix bath, which is the gelatin microgel-gelatin solution composite matrix bath in this study. While the diffusion of PVA is biocompatible with the cells embedded in the matrix, the diffusion of the cross-linking gelatin solution phase from the gelatin composite matrix into the sacrificial ink affects the final channel formation. The proposed Laponite nanoclay-modified PVA sacrificial composite ink is proved to have a reduced interdiffusivity due to the existence of the Laponite nanoclay-PVA network. The post-printing removability experiments show that the resulting PVA-Laponite nanoclay (typically less than 2.0%) composite ink is still easily water-dissolvable and can be removed by immersing in water, thus capable of creating perfusable patterns by removing embedded sacrificial patterns. The channel diameter

reduction due to the gelatin solution diffusion can be satisfactorily predicted based on the unidirectional diffusion model by using the 0.8% gelatin solution concentration as a threshold for gelatin removability during the sacrificial ink removal step. Overall, the improved printability, reduced post-printing interdiffusivity, and satisfactory post-printing ink removability of the Laponite-modified PVA sacrificial composite ink endow its potential for perfusable channel creation in thick tissue engineering applications.

Future work may include the experimental verification of the nanoclay "house-of-cards" microstructure and interactions between the PVA chain and Laponite nanoclay disc, the determination of the threshold of gelatin solution concentration for resulting gelatin gel to be removable, the understanding of the effect of Laponite nanoclay on the interdiffusion process during embedded printing, and the monitoring of lumen diameter change as a function of post-printing diffusion time and perfusion time. The reason that the study is conducted in a gelatin-based matrix bath is the gelatin is kept as part of the resulting construct after printing. As such, the study has focused on the printing performance in a biocompatible and biodegradable gelatin-based matrix bath. The feasibility of the PVA-Laponite nanoclay composite sacrificial ink for other applicable matrix bath materials should also be investigated. Furthermore, the resulting knowledge should be applicable to other sacrificial materials that can be bonded with Laponite nanoclay via different mechanisms such as electrostatically or via hydrogen bonds to improve the ink printability and reduce their interdiffusivity during embedded printing. In terms of applications towards tissue engineering, endothelization of the created channel by using the PVA-Laponite composite ink followed by vascular functionality investigations will be of great interest. This is critical for the creation of a 3D vascularized thick tissue model that can be used for disease

modeling, pathophysiology studies, and drug screening.

Author statement

Bing Ren: Conceptualization, Formal analysis, Writing-original draft, Methodology, Investigation, Writing-review & editing; **Kaidong Song**: Methodology, Writing-review & editing; **Yunxia Chen**: Methodology, Writing-review & editing; **Walter Lee Murfee**: Writing - review & editing; **Yong Huang**: Conceptualization, Project administration, Supervision, Writing-review & editing.

Declaration of competing interest

The authors declare that they have no conflicts to disclose.

Acknowledgments

This research was partially supported by the US National Science Foundation (1762941, 2233814) and the US National Institutes of Health (HL162405, U54CA233396, U54CA233444, & U54CA233465). The U54 grants support the Florida-California Cancer Research, Education and Engagement (CaRE2) Health Equity Center. The content is solely the responsibility of the authors and does not necessarily represent the official views of the National Institutes of Health. The final peer-reviewed manuscript is subject to the National Institutes of Health Public Access Policy. The use of the Anton Paar rheometers is also acknowledged.

Data Availability Statement

The data that support the findings of this study are available from the corresponding author upon reasonable request.

References

[1] Lovett M, Lee K, Edwards A, Kaplan DL. Vascularization Strategies for Tissue Engineering. Tissue Eng Part B Rev. 2009;15(3):353-70.
[2] Carmeliet P, Jain RK. Angiogenesis in cancer and other diseases. Nature. 2000;407(6801):249-57.
[3] Ren B, Jiang Z, Murfee WL, Katz AJ, Siemann D, Huang Y. Realizations of vascularized tissues: From in vitro platforms to in vivo grafts. Biophysics Reviews. 2023;4(1):011308.
[4] Mannino RG, Santiago-Miranda AN, Pradhan P, Qiu Y, Mejias JC, Neelapu SS, et al. 3D microvascular model recapitulates the diffuse large B-cell lymphoma tumor microenvironment in vitro. Lab on a chip. 2017;17(3):407-14.
[5] Neumann T, Nicholson BS, Sanders JE. Tissue engineering of perfused microvessels. Microvasc Res. 2003;66(1):59-67.
[6] Mandrycky C, Hadland B, Zheng Y. 3D curvature-instructed endothelial flow response and tissue vascularization. Sci Adv. 2020;6(38):eabb3629.
[7] Wang XY, Jin ZH, Gan BW, Lv SW, Xie M, Huang WH. Engineering interconnected 3D vascular networks in hydrogels using molded sodium alginate lattice as the sacrificial template. Lab on a chip. 2014;14(15):2709-16.
[8] Tocchio A, Tamplenizza M, Martello F, Gerges I, Rossi E, Argentiere S, et al. Versatile fabrication of vascularizable scaffolds for large tissue engineering in bioreactor. Biomaterials. 2015;45:124-31.
[9] Kolesky DB, Homan KA, Skylar-Scott MA, Lewis JA. Three-dimensional bioprinting of thick vascularized tissues. P Natl Acad Sci USA. 2016;113(12):3179-84.
[10] Kinstlinger IS, Saxton SH, Calderon GA, Ruiz KV, Yalacki DR, Deme PR, et al. Generation of model tissues with dendritic vascular networks via sacrificial laser-sintered carbohydrate templates. Nat Biomed Eng. 2020;4(9):916-32.
[11] Homan KA, Kolesky DB, Skylar-Scott MA, Herrmann J, Obuobi H, Moisan A, et al. Bioprinting of 3D Convoluted Renal Proximal Tubules on Perfusable Chips. Sci Rep. 2016;6(1):34845.
[12] Hu M, Dailamy A, Lei XY, Parekh U, McDonald D, Kumar A, et al. Facile Engineering of Long-Term Culturable Ex Vivo Vascularized Tissues Using Biologically Derived Matrices. Adv Healthc Mater. 2018;7(23):e1800845.
[13] Huang Y, Leu MC, Mazumder J, Donmez A. Additive Manufacturing: Current State, Future Potential, Gaps and Needs, and Recommendations. J Manuf Sci E. 2015;137(1):014001.
[14] Huang Y, Schmid SR. Additive Manufacturing for Health: State of the Art, Gaps and Needs, and Recommendations. J Manuf Sci E. 2018;140(9).
[15] Lee VK, Kim DY, Ngo H, Lee Y, Seo L, Yoo SS, et al. Creating perfused functional vascular channels using 3D bio-printing technology. Biomaterials. 2014;35(28):8092-102.
[16] Zhao L, Lee VK, Yoo SS, Dai G, Intes X. The integration of 3-D cell printing and mesoscopic fluorescence molecular tomography of vascular constructs within thick hydrogel scaffolds. Biomaterials. 2012;33(21):5325-32.
[17] Brandenberg N, Lutolf MP. In Situ Patterning of Microfluidic Networks in 3D Cell-Laden Hydrogels. Adv Mater. 2016;28(34):7450-6.
[18] Arakawa CK, Badeau BA, Zheng Y, DeForest CA. Multicellular Vascularized Engineered Tissues through User-Programmable Biomaterial Photodegradation. Adv Mater. 2017;29(37):1703156.
[19] Hofer M, Lutolf MP. Engineering organoids. Nature reviews Materials. 2021;6(5):402-20.
[20] Skylar-Scott MA, Uzel SG, Nam LL, Ahrens JH, Truby RL, Damaraju S, et al. Biomanufacturing of organ-specific tissues with high cellular density and embedded vascular channels. Sci Adv. 2019;5(9):eaaw2459.
[21] Compaan AM, Song K, Chai W, Huang Y. Cross-Linkable Microgel Composite Matrix Bath for Embedded Bioprinting of Perfusable Tissue Constructs and Sculpting of Solid Objects. ACS Appl Mater Interfaces. 2020;12(7):7855-68.
[22] Wu Q, Song K, Zhang D, Ren B, Sole-Gras M, Huang Y, et al. Embedded extrusion printing in

yield-stress-fluid baths. Matter. 2022;5(11):3775-806.
[23] Grigoryan B, Paulsen SJ, Corbett DC, Sazer DW, Fortin CL, Zaita AJ, et al. Multivascular networks and functional intravascular topologies within biocompatible hydrogels. Science. 2019;364(6439):458-64.
[24] Zhu W, Qu X, Zhu J, Ma X, Patel S, Liu J, et al. Direct 3D bioprinting of prevascularized tissue constructs with complex microarchitecture. Biomaterials. 2017;124:106-15.
[25] Lian L, Zhou C, Tang G, Xie M, Wang Z, Luo Z, et al. Uniaxial and Coaxial Vertical Embedded Extrusion Bioprinting. Adv Healthc Mater. 2022;11(9):e2102411.
[26] Cheng F, Cao X, Li H, Liu T, Xie X, Huang D, et al. Generation of Cost-Effective Paper-Based Tissue Models through Matrix-Assisted Sacrificial 3D Printing. Nano Lett. 2019;19(6):3603-11.
[27] Miller JS, Stevens KR, Yang MT, Baker BM, Nguyen DH, Cohen DM, et al. Rapid casting of patterned vascular networks for perfusable engineered three-dimensional tissues. Nat Mater. 2012;11(9):768-74.
[28] Bertassoni LE, Cecconi M, Manoharan V, Nikkhah M, Hjortnaes J, Cristino AL, et al. Hydrogel bioprinted microchannel networks for vascularization of tissue engineering constructs. Lab on a chip. 2014;14(13):2202-11.
[29] Li S, Liu YY, Liu LJ, Hu QX. A Versatile Method for Fabricating Tissue Engineering Scaffolds with a Three-Dimensional Channel for Prevasculature Networks. ACS Appl Mater Interfaces. 2016;8(38):25096-103.
[30] Ahlfeld T, Kohler T, Czichy C, Lode A, Gelinsky M. A Methylcellulose Hydrogel as Support for 3D Plotting of Complex Shaped Calcium Phosphate Scaffolds. Gels. 2018;4(3):68.
[31] Compaan AM, Christensen K, Huang Y. Inkjet Bioprinting of 3D Silk Fibroin Cellular Constructs Using Sacrificial Alginate. ACS Biomater Sci Eng. 2017;3(8):1519-26.
[32] Li H, Cheng F, Li W, Cao X, Wang Z, Wang M, et al. Expanding sacrificially printed microfluidic channel-embedded paper devices for construction of volumetric tissue models in vitro. Biofabrication. 2020;12(4):045027.
[33] Escobar-Chávez JJ, López-Cervantes M, Naïk A, Kalia YN, Quintanar-Guerrero D, Ganem-Quintanar A. Applications of thermo-reversible pluronic F-127 gels in pharmaceutical formulations. J Pharm Pharm Sci. 2006;9(3):339-58.
[34] Xia Y, Zhang X, Bo A, Sun J, Li M. Sodium citrate inhibits the proliferation of human gastric adenocarcinoma epithelia cells. Oncol Lett. 2018;15(5):6622-8.
[35] Pimentel CR, Ko SK, Caviglia C, Wolff A, Emneus J, Keller SS, et al. Three-dimensional fabrication of thick and densely populated soft constructs with complex and actively perfused channel network. Acta Biomater. 2018;65:174-84.
[36] Dawson JI, Kanczler JM, Yang XB, Attard GS, Oreffo RO. Clay gels for the delivery of regenerative microenvironments. Adv Mater. 2011;23(29):3304-8.
[37] Tomas H, Alves CS, Rodrigues J. Laponite(R): A key nanoplatform for biomedical applications? Nanomedicine : nanotechnology, biology, and medicine. 2018;14(7):2407-20.
[38] Gaharwar AK, Mihaila SM, Swami A, Patel A, Sant S, Reis RL, et al. Bioactive Silicate Nanoplatelets for Osteogenic Differentiation of Human Mesenchymal Stem Cells. Adv Mater. 2013;25(24):3329-36.
[39] Jin Y, Liu C, Chai W, Compaan A, Huang Y. Self-Supporting Nanoclay as Internal Scaffold Material for Direct Printing of Soft Hydrogel Composite Structures in Air. ACS Appl Mater Interfaces. 2017;9(20):17456-65.
[40] Jin Y, Shen Y, Yin J, Qian J, Huang Y. Nanoclay-Based Self-Supporting Responsive Nanocomposite Hydrogels for Printing Applications. ACS Appl Mater Interfaces. 2018;10(12):10461-70.
[41] Ma Z, He H, Deng C, Ren Y, Lu D, Li W, et al. 3D bioprinting of proangiogenic constructs with induced immunomodulatory microenvironments through a dual cross-linking procedure using laponite incorporated bioink. Compos B Eng. 2022;229:109399.
[42] Song K, Ren B, Zhai Y, Chai W, Huang Y. Effects of transglutaminase cross-linking process on printability of gelatin microgel-gelatin solution composite bioink. Biofabrication. 2021;14(1).
[43] Compaan AM, Song K, Huang Y. Gellan Fluid Gel as a Versatile Support Bath Material for Fluid

Extrusion Bioprinting. ACS Appl Mater Interfaces. 2019;11(6):5714-26.
[44] Davila JL, d'Avila MA. Laponite as a rheology modifier of alginate solutions: Physical gelation and aging evolution. Carbohydrate polymers. 2017;157:1-8.
[45] Ruzicka B, Zaccarelli E. A fresh look at the Laponite phase diagram. Soft Matter. 2011;7(4):1268.
[46] Selim A, Toth AJ, Fozer D, Suvegh K, Mizsey P. Facile Preparation of a Laponite/PVA Mixed Matrix Membrane for Efficient and Sustainable Pervaporative Dehydration of C1-C3 Alcohols. ACS omega. 2020;5(50):32373-85.
[47] de Oliveira MJA, Parra DF, Amato VS, Lugão AB. Hydrogel membranes of PVAl/ clay by gamma radiation. Radiation Physics and Chemistry. 2013;84:111-4.
[48] Morariu S, Bercea M, Brunchi CE. Influence of Laponite RD on the properties of poly(vinyl alcohol) hydrogels. Journal of Applied Polymer Science, . 2018;135(35):46661.
[49] Herrera NN, Letoffe J-M, Reymond J-P, Bourgeat-Lami E. Silylation of laponite clay particles with monofunctional and trifunctional vinyl alkoxysilanes. Journal of Materials Chemistry. 2005;15(8):863.